ELSEVIER

Contents lists available at ScienceDirect

### Aquaculture

journal homepage: www.elsevier.com/locate/aquaculture





# Gckr depletion leads to growth retardation and diet-dependent visceral obesity in red crucian carp (*Carassius auratus* red var.)

Juan Li<sup>a</sup>, Huilin Li<sup>a</sup>, Yuan Ou<sup>a</sup>, Qiyong Lou<sup>b</sup>, Zehong Wei<sup>a</sup>, Ming Wen<sup>a</sup>, Shi Wang<sup>a</sup>, Qingfeng Liu<sup>a</sup>, Yuqin Shu<sup>a,\*</sup>, Shaojun Liu<sup>a</sup>

- <sup>a</sup> State Key Laboratory of Developmental Biology of Freshwater Fish, Engineering Research Center of Polyploid Fish Reproduction and Breeding of the State Education Ministry, College of Life Sciences, Hunan Normal University, Changsha 410081, Hunan, China
- b State Key Laboratory of Freshwater Ecology and Biotechnology, Institute of Hydrobiology, Chinese Academy of Sciences, Wuhan 430072, Hubei, China.

#### ARTICLE INFO

Keywords:
Gckr
Gck
Insulin
Glycolysis
Lipid metabolism

#### ABSTRACT

There exists a notable contrast in the carbohydrate utilization capacity between fish and mammals. In mammals, the glucokinase regulatory protein (GCKR) is known to exert inhibitory effects on glycolysis by binding to glucokinase (GCK), but its role in fish remains unexplored. In this study, the function of gckr in red crucian carp (Carassius auratus red var.), hereafter referred to as RCC, was investigated through its knockout. Under normal dietary conditions, the growth rate of gckr knockout RCC was significantly lower compared to wild-type (WT) RCC reared in the same environment. Subsequent analysis found that gckr knockout RCC exhibited significantly higher serum glucose levels at 1 h post-feeding or glucose injection (hpi), while the difference was abolished at 3 h. Therefore, the metabolic characteristics at 1 and 3 hpi were evaluated between WT and gckr knockout RCC. The results revealed that gckr knockout led to impaired insulin signaling and glycolysis, as evidenced by a reduction in serum insulin level, hepatic insulin receptor a and pyruvate kinase expression, GCK contents, and pyruvate levels at 1 hpi. Additionally, gckr knockout resulted in compromised gluconeogenesis, as indicated by a significant decrease in hepatic expression of fructose-1,6-bisphosphatase 1 and glucose-6-phosphatase at 1 hpi, while it did not affect glycogen accumulation after glucose injection. Regarding lipid metabolism, gckr knockout caused a transient decrease in triglyceride level and reduced expression of fatty acid synthase after glucose injection. Moreover, decreased hepatic peroxisome proliferator activated receptor alpha (ppara) transcripts and proteins were observed in gckr knockout RCC at 1 dpi, indicating a reduced capacity for β-oxidation due to Gckr deficiency. Interestingly, when fed a high-lipid diet, gckr knockout resulted in a significant increase in visceral mass with higher triglyceride level, accompanied by attenuated PPARa signaling. Taken together, this study provides evidence that Gckr-mediated maintenance of Gck contributes to the facilitation of postprandial glycolysis, gluconeogenesis, lipogenesis, and fatty acid β-oxidation in RCC. This study further suggests that enhancing glycolysis may promote growth and liver health in fish under high lipid dietary conditions.

#### 1. Introduction

Glucokinase (hexokinase IV or D, GCK) initiates glycolysis by catalyzing the phosphorylation of glucose to glucose 6-phosphate (G6P) and therefore plays an important role in the regulation of blood glucose (Sternisha and Miller, 2019). Glucokinase regulator (GCKR), also known as glucokinase regulatory protein, was first identified by Van Schaftingen in 1989 as an inhibitor of GCK by inducing a lower affinity for glucose phosphorylation *in vivo* (van Schaftingen et al., 1997). The

binding of GCKR to GCK in liver downregulated its affinity for glucose, leading to inhibition of glycolysis (Detheux et al., 1991). Mammalian GCKR belongs to the sugar isomerase (ISI) family, which is predominantly expressed in the liver. The N-terminal SIS domain contains the binding sites for fructose 6-phosphate (F6P) and fructose 1-phosphate (F1P), while the C-terminal domain possesses the binding site for GCK (Veiga-da-Cunha et al., 2009). By taking advantage of creating different mutants of rat GCKR and determining their affinity and the activity of GCK, it was determined that GCKR has a single binding site for

E-mail address: shuyuqin@hunnu.edu.cn (Y. Shu).

<sup>\*</sup> Corresponding author at: State Key Laboratory of Developmental Biology of Freshwater Fish, College of Life Sciences, Hunan Normal University, 36 Lushan Road, Changsha 410081, P.R. China.

phosphate esters (Veiga-da-Cunha and Van Schaftingen, 2002). Crystal structure analysis of GCKR further revealed that the competitive binding site between F1P and F6P is buried deep within a domain interface (Pautsch et al., 2013). The binding affinity between GCKR and GCK is enhanced by binding to F6P, whereas it is diminished by binding to F1P (Brown et al., 1997; Detheux et al., 1991).

The knowledge of GCKR's role *in vivo* mainly comes from GCKR-deficient mice. Despite a significant reduction in hepatic GCK levels in GCKR-deficient mice, the GCK activity in the liver homogenates remained unchanged. However, the GCKR-deficient mice displayed tardive glucose clearance in the glucose tolerance test (Grimsby et al., 2000). Conversely, overexpression of GCKR in mice improved glucose tolerance and reduced fasting blood glucose levels, accompanied by decreased insulin levels (Slosberg et al., 2001). These results suggest both a regulatory and a stabilizing role for GCKR in the mammalian liver.

The consumption of a diet rich in carbohydrates often leads to the manifestation of persistent postprandial hyperglycemia in fish, highlighting a diminished ability for effective glucose utilization (Enes et al., 2009; Moon, 2001; Wilson, 1994). Notably, all glycolytic enzymes have been reported to be present in fish (Walton and Cowey, 1982). In a pioneering study conducted by Soengas et al. in 2009, the existence of GCKR-like proteins with molecular weights approximately 68 kDa was demonstrated in rainbow trout, carp, and goldfish, and their expression was detected in the liver. These GCKR-like proteins exhibited functional similarity to mammalian GCKR. Comparisons of GCKR-like protein properties among different teleost species revealed that the most intolerant species possessed the most potent GCKR-like protein, while tolerant species displayed minimal binding of GCK and GCKR (Polakof et al., 2009). Remarkably, while GCK is highly conserved from fish to mammals, GCKR exhibits variability across species. Whether the variation of GCKR leads to differences in the ability to utilize carbohydrates in fish? Whereas the function of gckr remains unexplored in fish.

In this study, we generated gckr knockout RCC and investigated the effects of Gckr depletion on growth, glucose metabolism, and lipid metabolism. The results revealed that gckr knockout out led to tardy glucose clearance and stunted growth, possibly resulting from compromised glycolysis and the induced impairment of insulin signaling. Gckr depletion also resulted in reduced gluconeogenesis, lipid synthesis, and Ppara signaling. These perturbations further precipitated an increase in visceral mass, elevated triglyceride levels, and augmented fat accumulation under conditions of a high carbohydrate diet. Our findings, therefore, signify that the initial step of glycolysis catalyzed by GCK provides a driving force for growth, lipid synthesis, and fatty acid  $\beta$ -oxidation in fish.

### 2. Materials and methods

#### 2.1. Ethics statement

We followed the laboratory animal guideline for the ethical review of the animal welfare of China (GB/T 35,892–2018). Before sampling, fish were euthanized with tricaine methanesulfonate (A5040-25G, Sigma) at a concentration of 100 mg/L. All animal experiments in this study were approved by the Institutional Animal Care and Use Committee of Hunan Normal University (Permit Number: 630).

#### 2.2. Generation of gckr knockout RCC

Based on CRISPR/Cas9 strategy, the target was designed on the third exon of gckr and the sequence is as follows: GATGGTGGATGTTG-CAAAGA. The gRNA was synthesized using TranscriptAid T7 high-yield transcription kits (K0441, Thermo Scientific Fermentas, Waltham, MA, United States of America), and the Cas9 mRNA was transcribed using the mMESSAGE mMACHINE<sup>TM</sup> T3 Transcription kit (AM1348 Ambion, Austin, TX, USA). The mixture containing 50 ng/ $\mu$ L gRNA and 100 ng/

 $\mu$ L *Cas9* mRNA was injected into one to four cell stage embryos. The targeted regions were amplified using the following primers listed in Table S1 and sequenced to confirm the mutation. Homozygous RCC were generated by self-crossing heterozygotes carrying identical mutations.

#### 2.3. Growth performance assay

WT and gckr knockout RCC were initially reared in separate ponds. To conduct this experiment, we assessed the weights of all fish in both ponds and handpicked 30 individuals from each group, with an initial weight averaging  $0.94 \pm 0.19$  g. When the experimental fish were selected, they were mixed and reared in one net cage to be kept in completely same conditions. The experimental fish were fed twice daily at 9:00 and 18:00 with the satiation feeding strategy. For normal dietary conditions, the experimental fish were fed with commercial crucian carp feed. For treatment, the experimental fish were fed with a formulated diet containing 8.8% lipid. The formulation of the experimental highlipid diet was based on a previous study (Tan et al., 2009), and the feed formula was shown in Table S2. The approximate composition of two diets were measured according to the procedures of the Association of Official Analytical Chemists (Baur and Ensminger, 1977). Dry matter was measured at 105 °C to constant weight. Crude protein was determined using a full-automatic Kjeldahl tester (K-9840, Hanon, China). Crude lipid was determined through the Soxhlet extraction method after initial extraction with petroleum ether. Ash was measured after being burned at 550 °C for 3 h in a muffle furnace (GBT6438-2007). The carbohydrate content of the feed was determined by subtracting crude protein, crude fat, and ash from the dry matter. The approximate composition of two diets was shown in Table S3. The feeding trial lasted for 8 weeks, after which the WT and gckr knockout RCC were identified by genotyping with primers listed in Table S1, and their weights and lengths were measured and analyzed to compare their growth performance.

#### 2.4. Glucose treatment and serum glucose assay

In the glucose challenge test, both oral feeding and intravenous glucose injection were attempted to assess the response to elevated blood sugar levels. Fifty-one WT and fifty-three gckr knockout RCC were fasted for 24 h (h) and this time point was considered as 0 h. For the feeding strategy, satiation feeding was started at 0 h point and completed within 30 min. For the injection strategy, the experimental fish were injected with 250 mg/mL glucose dissolved in sterile saline at a concentration of 500 mg per kilogram, and the injection of two groups was performed simultaneously and completed within 30 min. The concentration of glucose for injection was according to a previous study (Jin et al., 2018). About 0.1 mL blood was drawn from the tail vein of treated fish at 0 h, 1 h, 3 h, 6 h, and 24 h after treatment, and the blood glucose levels were determined using a glucose meter (Performa, Roche, Switzerland). Each fish was sampled once and these experimental fish were trained to reduce the stress response by multiple harvests prior to the experiment.

## 2.5. Assay of serum insulin using enzyme-linked immunosorbent assay (ELISA) kit

Blood was drawn from the tail vein of the experimental fish and allowed to clot naturally for 20 min at room temperature. The blood was then centrifuged at 2000 rpm for 20 min and the supernatant was carefully collected. The Insulin Assay kit (H203–1-1, Nanjing jiancheng Bioengineering Institute, China) was used to determine the insulin content and the procedure was performed according to the kit instructions. The OD values of the samples were determined using a microplate reader (Synergy2, BioTek, USA). Three replicates were made for each sample and the average of the three values represents the

individual sample value. Ten individuals per group were used for this assay.

#### 2.6. Determination of GCK content using ELISA kit

Approximately 0.1 g of liver or muscle was collected as a sample and added with 9 volumes of phosphate buffered saline, thoroughly homogenized, and centrifuged at 2000 rpm for 20 min. The supernatant was then carefully collected and 10  $\mu$ L aliquot was used to determine the protein concentration using a spectrophotometer (UV-1100, MAPADA, China) according to the Total Protein Assay kit (A045-4-2, Nanjing jiancheng Bioengineering Institute, China). The remain supernatant was stored at  $-20\,^{\circ}\text{C}$  until assayed. The GCK content of the supernatant was measured using the Glucokinase Assay kit (H439-1, Nanjing jiancheng Bioengineering Institute, China) and the procedure was performed according to the instructions provided with the kit. The OD values of the samples were determined using a microplate reader (Synergy2, BioTek, USA). The final pyruvate content in liver and muscle was normalized to the total protein content. Three replicates were made for each sample and the average of the three values represents the individual sample value. Six individuals per group were used for this assay.

#### 2.7. Assay of pyruvate in serum and tissue

For the measurement of serum pyruvate, the blood sample was treated as in 2.4. For the measurement of pyruvate in tissues, approximately 0.1 g of liver or muscle was taken as a sample and added with 9 volumes of pre-cooled physiological saline, homogenized in an ice-water bath, centrifuged at 2500 rpm for 10 min and the supernatant carefully collected. A portion of the supernatant was then taken to determine the protein concentration using a spectrophotometer (UV-1100, MAPADA, China) according to the Total Protein Assay kit (A045-4-2, Nanjing jiancheng Bioengineering Institute, China), and the remainder was used to determine pyruvate. Pyruvates in both serum and tissue were determined with the Pyruvate Assay kit (A081-1-1, Nanjing jiancheng Bioengineering Institute, China) on a Microplate Reader (Synergy2, BioTek, USA). According to the kit instructions, the final pyruvate content in liver or muscle was normalized to the total protein content. Three replicates were set up for each sample and the average of the three values represented the individual sample value. Six individuals per group were used for this assay.

#### 2.8. Assay of glycogen in liver and muscle

Approximately 0.1 g of liver or muscle was digested with three volumes of alkali solution, heated in a boiling water bath for 20 min and cooled under running water. Then, the liver and muscle hydrolysis solutions were prepared into 1% and 5% detection solution, respectively, and then assayed under a spectrophotometer (UV-1100, MAPADA, China) according to the Glycogen Assay kit (A043–1-1, Nanjing jiancheng Bioengineering Institute, China). Based on the detected OD values, the glycogen content was calculated according to the formula in the instructions. Three replicates were made for each sample and the average of the three values represents the individual sample value. For this assay, six individuals were used for each group.

#### 2.9. Assay of triglyceride in serum and tissue

The preparation of serum was the same as that of insulin detection. For liver preparation, an approximate 0.1 g tissue was added with 9 volumes of anhydrous ethanol, homogenized under ice-water bath conditions, centrifuged at 2500 rpm for 10 min, and the supernatant was collected carefully. For muscle preparation, the phosphate-buffered saline substituted anhydrous ethanol as homogenate medium, and the rest procedures were the same as the preparation of liver samples. All the samples were assayed with a spectrophotometer (UV-1100, MAPADA,

China) according to the Triglyceride Assay kit (A110–2-1, Nanjing jiancheng Bioengineering Institute, China). Three replicates were set up for each sample and the average of the three values represented the individual sample value. Six individuals per group were used for this assay.

#### 2.10. Total RNA extraction and quantitative PCR (q-PCR)

Total RNA was extracted from the liver and muscle of WT and gckr knockout RCC using the Trizol reagent (15596026CN, Invitrogen). All tissues were fully homogenized under ice bath conditions. The homogenates were then mixed with chloroform, centrifuged at 12000 rmp for 10 min and the aqueous phase was carefully collected. Isopropyl alcohol was added and the resulting floc became a white precipitate after centrifugation. The RNA precipitate was then washed with 75% ethanol, dried at room temperature and dissolved in DEPC water. The obtained RNA was then treated with DNase to remove DNA contamination, repurified by phenol-chloroform extraction and redissolved in 50  $\mu$ L DEPC water. The resulting RNA was subjected to reverse transcription using the Revert-Aid First Strand cDNA Synthesis kit (Thermo-Fisher Scientific, USA), and the synthesized cDNA was used as a template for q-PCR with the primers listed in Table S1. The q-PCR was performed using the SYBR Green (MQ00601S, Monad, China) method on a Real-Time PCR System (Quantstudio 5, ABI, USA), and the relative expression levels of the target genes were normalized to the expression level of gapdh. Three replicates were set up for each sample, and six individuals were used for each group. The qPCR results are analyzed for significance using t-test.

#### 2.11. Western blotting

Approximately 5 mg of liver or muscle was put into 1.5 mL eppendorf tube, added with 500 µL RIPA lysis buffer (P0013B, Beyotime, China) containing protease and phosphatase inhibitor cocktail (P1046, Beyotime, China), and freshly added phenylmethylsulfonyl fluoride (ST506, Beyotime, China). After incubation on ice for 10 min, the samples were thoroughly homogenized, sonicated several times until clear and transparent, and centrifuged at 12,000 rpm (4 °C) for 5 min. The supernatants were then collected, mixed with an equal volume of  $2\times$ sample buffer and boiled for 5 min. The prepared samples were subjected to sodium dodecyl sulfate-polyacrylamide gel electrophoresis (SDS-PAGE), transblotted onto a nylon membrane, blocked, sequentially incubated in the primary and secondary antibodies, and exposed to Western Blotting Substrate (Thermo Fisher Scientific, #32109). Finally, the signals were detected using a chemiluminescence imaging system (Chemidoc, Bio-Rad, USA). The primary antibodies against glyceraldehyde-3-phosphate dehydrogenase (Gapdh, MA5-15738, Invitrogen), ribosomal protein S6 kinase (S6, 2217S, Cell Signaling Technology), phosphorylated ribosomal protein S6 kinase (pS6, 4858S, Cell Signaling Technology), and Ppara (A24835, ABclonal), and the secondary antibodies of HRP-conjugated goat anti-mouse immunoglobulin G (D110098, Sangon Biotech) and HRP-conjugated goat antirabbit IgG (D110058, Sangon Biotech) were used in this study.

#### 2.12. Histological section preparation and HE staining

The tissues were fixed in Bouin solution (PH0976, Phygene, China) for over 24 h and then subjected to the standard procedures (Zhang et al., 2021) as follows: dehydrated with a graded series of ethanol (70%, 80%, 90%, 95%, and 100% ratios), permeabilized in a mixture of xylene and ethanol at a ratio of 1:1 for 45 min and xylene only for 15 min, embedded in paraffin wax, sliced at 8  $\mu$ m thickness and placed on slides, baked at 42 °C overnight, dewaxed in xylene, rehydrated in gradient ethanol with 100%, 95%, 90%, 80%, and 70% ratios, stained in hematoxylin for 30 s, washed with ddH<sub>2</sub>O, treated with 0.5% HCl and 0.2% NaOH respectively, stained in eosin for 2 min and finally sealed with

glycerol resin.

J. Li et al.

#### 2.13. Oil red stanning

Liver tissues were fixed in 4% paraformaldehyde (E672002, Sangon Biotech, China) for over 24 h and then subjected to the following procedures: Dehydrated in 30% sucrose solution overnight at 4  $^{\circ}$ C, permeabilized with optimal cutting temperature compound and embedded, prepared into ice slices and placed on slides, rewarmed at room temperature and washed with ddH<sub>2</sub>0, permeated with 60% isopropanol for 2 min, stained with oil red working solution (G1015-100ML, Servicebio, China) for 8 min, rinsed with 60% isopropanol for 3 s, washed with pure water, stained with hematoxylin for 30 s, and finally sealed with glycerol resin after washing, blue recovery, washing, and drying. The observations were conducted under a Leica microscope (DM2500, Leica, Germany).

#### 2.14. Transcriptome analyses

Testes were isolated from males and immediately placed on dry ice. Total RNA was extracted with TRIzol reagent (Ambion, 15,596, USA). RNA integrity was assessed using the RNA Nano 6000 Assay kit of the Bioanalyzer 2100 system (Agilent Technologies, CA, USA). The RNA-seq was performed on an Illumina Novaseq platform and 150 bp paired-end reads were generate. Clean reads were mapped to the goldfish genome

(ASM336829v1) using Hisa2 v2.0.5. The KEGG pathway enrichment analysis was performed using the clusterProfiler R package, considering differentially expressed genes with a corrected P-value of <0.05.

#### 2.15. Statistical analysis

An evaluation was performed to assess the normal distribution of parameters derived from WT and *gckr* knockout RCC. Parameters demonstrating normality were subjected to the independent-samples *t*-test, while those failing to meet normality criteria were analyzed using the Kruskal-Wallis test. Both t-test and Kruskal-Wallis test were conducted using IBM SPSS Statistics for Windows, version 27.0 (IBMCorp., Armonk, N.Y., USA). All parameters in this study, such as body weight, insulin level, gene expression, serum glucose, GCK content, pyruvate content/level, glycogen content, triglyceride content/level, *ppara* transcripts and ratios of visceral mass, followed an approximately normal distribution. All the results are presented as mean  $\pm$  standard error ( $n \ge 3$ ). The results were considered statistically significant at P < 0.05.

#### 3. Results

#### 3.1. Gckr depletion inhibited growth and insulin signaling

The *gckr* gene in RCC consists of 19 exons and the knockout target was designed on the third exon. We successfully generated two knockout

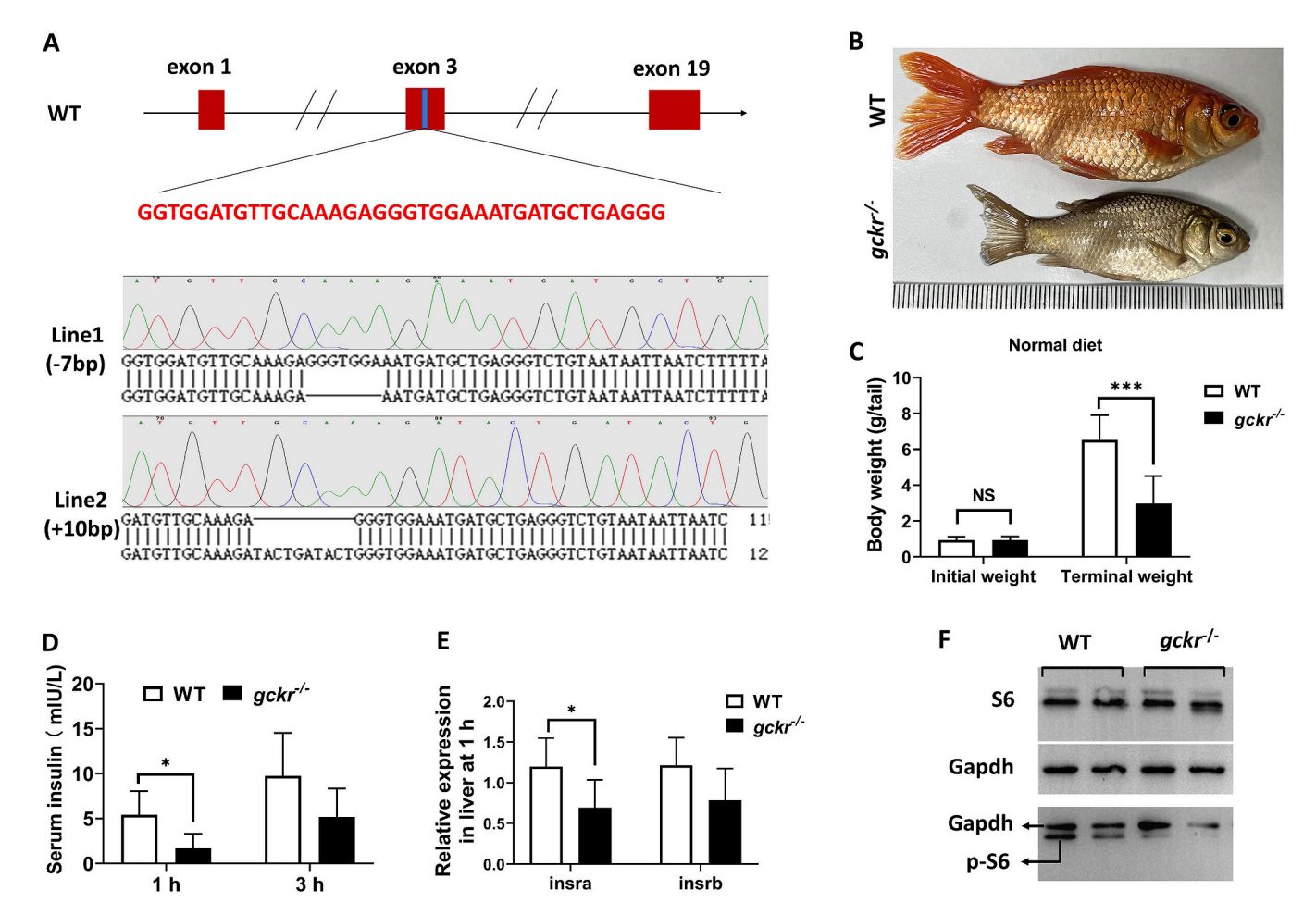


**Fig. 1.** *Gckr* knockout led to reduced growth and compromised insulin signaling in RCC. (A) Target design and the blast results of mutant *gckr* sequences. (B) Typical appearance of WT and *gckr* knockout RCC after feeding trial with same initial weight. (C) Statistic analysis of initial and terminal body weight of WT and *gckr* knockout RCC during the feeding trial. (D) Serum insulin levels of WT and *gckr* knockout RCC at 1 and 3 h post glucose injection (hpi). (E) Expression levels of insulin receptors in livers of WT and *gckr* knockout RCC at 1 hpi. (F) Western blot analysis of S6 and p-S6 proteins from liver tissue of WT and *gckr* knockout RCC fish. GAPDH protein was used as the reference.

J. Li et al. Aquaculture 592 (2024) 741245

lines with a 7-base deletion and a 10-base insertion, respectively (Fig. 1A). The experimental data in this study were mainly collected from the 10-base insertion line. WT and gckr knockout RCC with the same initial body weight were selected for the feeding trial. After 8 weeks, gckr knockout RCC showed obviously smaller body size than WT RCC, while there was no visible difference in the appearance between them (Fig. 1B). After weighing, it was determined that WT RCC had significantly higher terminal body weight than gckr knockout RCC (Fig. 1C). Given the role of insulin signaling in glucose metabolism and growth, we further investigated whether it was altered due to gckr knockout. It was found that gckr knockout RCC exhibited significantly lower serum insulin levels (Fig. 1D) and downregulated the expression of insulin receptor a (insra) in liver (Fig. 1E) at 1 hpi. Consistently, western blot revealed that activation of the downstream effect factor S6, in the form of phosphorylated S6, was impaired in gckr knockout RCC at 1 hpi (Fig. 1F). These results suggest that gckr knockout impairs postprandial insulin signaling and thereby inhibits the growth.

## 3.2. Gckr depletion caused compromised glycolysis and gluconeogenesis in $\it RCC$

To investigate the effect of *gckr* knockout on serum glucose in RCC, we conducted both feeding and intraperitoneal glucose injection. Both treatments were performed with 24 h of starvation as the starting point of the cycle (0 h), and the serum glucose levels of the two groups of RCC

were continuously monitored at 0 h, 1 h, 3 h, 6 h, and 24 h after treatment. The results showed that the trends in serum glucose changes obtained from the two treatments were consistent. At the 0-1 h stage, both WT and gckr knockout RCC showed an increasing trend in serum glucose after feeding/intraperitoneal glucose injection, reaching peak at 1 h after both treatments. However, gckr knockout RCC displayed faster rise in serum glucose, and reached a significantly higher peak compared to WT RCC. At the 1-3 h stage, gckr knockout RCC showed a faster decrease in serum glucose level, while WT RCC displayed only a slight decline. Therefore, the difference in serum glucose level between WT and gckr knockout RCC was eliminated at 3 h post treatment. During the  $3-24\,h$  period, both groups showed little variation and a general trend of gradual decrease in serum glucose (Fig. 2A and B). It can be concluded that the differences in serum glucose between WT and gckr knockout RCC were mainly concentrated 0-3 h after feeding/intraperitoneal glucose injection. Therefore, the subsequent investigation of other physiological and biochemical indices was focused on 1 and 3 h after glucose injection.

Considering the established interaction between Gck and Gckr, we examined Gck levels in both WT and *gckr* knockout RCC using an ELISA kit. The results found that WT RCC had significantly higher hepatic Gck contents at 1 hpi, and the difference was absent at 3 hpi (Fig. 2C). This finding suggests that the binding of Gckr to Gck functions as maintenance, stabilization, or storage of Gck, which may be in a rapid response to the increase in serum glucose. Given that Gck is the rate-limiting

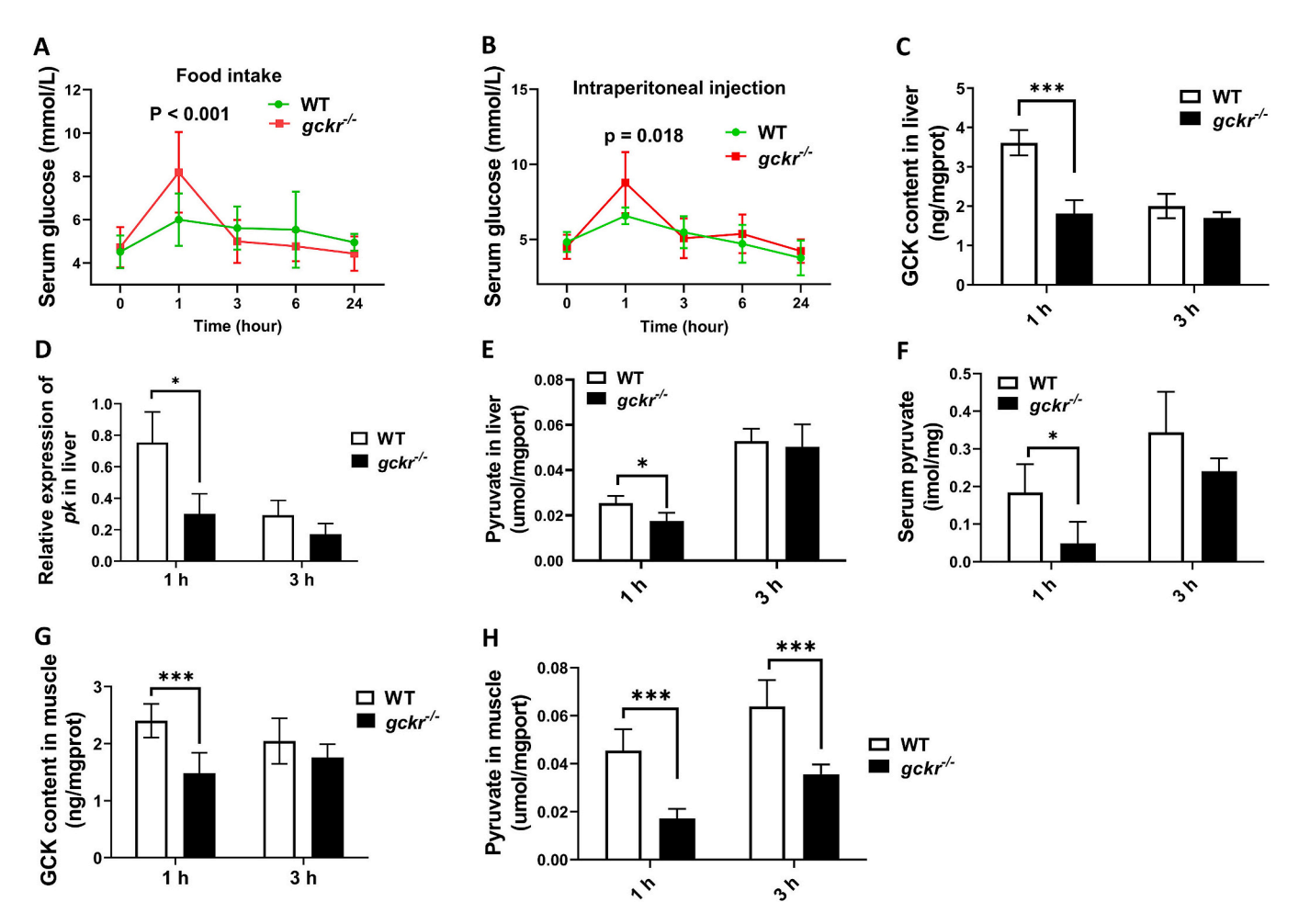


**Fig. 2.** *Gckr* knockout led to impaired glucose clearance and compromised glycolysis post glucose challenge in RCC. (A) Blood glucose levels of WT and *gckr* knockout RCC at 0, 1, 3, 6, and 24 h after food intake. (B) Blood glucose levels of WT and *gckr* knockout RCC at 0, 1, 3, 6, and 24 hpi. (C) GCK content in livers of WT and *gckr* knockout RCC at 1 and 3 hpi. (D) Expression levels of *pk* in livers of WT and *gckr* knockout RCC at 1 and 3 hpi. (E) Pyruvate contents in livers of WT and *gckr* knockout RCC at 1 and 3 hpi. (F) Serum pyruvate contents of WT and *gckr* knockout RCC at 1 h, 3 h and 6 h post glucose injection. (G) GCK content in muscle of WT and *gckr* knockout RCC at 1 and 3 hpi. (H) Pyruvate contents in muscle of WT and *gckr* knockout RCC at 1 and 3 hpi.

J. Li et al. Aquaculture 592 (2024) 741245

enzyme in the first step of glycolysis, the other indices related to glycolysis were examined. The results revealed that *gckr* knockout RCC had significantly lower hepatic expression of *pk*, which was another ratelimiting enzyme in glycolysis, at 1 hpi (Fig. 2D). Correspondingly, *gckr* knockout RCC also showed significantly decreased hepatic pyruvate contents and serum pyruvate levels at 1 hpi (Fig. 2E and F). Similar trends were also observed in the muscle of *gckr* knockout RCC, which had significantly lower Gck levels at 1 hpi (Fig. 2G) and reduced pyruvate contents at both 1 and 3 hpi (Fig. 2H). These results strongly suggest that *gckr* knockout impairs the postprandial glycolysis in RCC.

Gluconeogenesis and glycogen accumulation also play an important

role in the regulation of postprandial glucose. Therefore, we also investigated whether there were differences in gluconeogenesis or glycogen accumulation between WT and *gckr* knockout RCC. The results revealed that the expression of *fbpase* and *g6pase*, the key enzymes related to gluconeogenesis, were dramatically downregulated in *gckr* knockout RCC at 1 hpi, but showed no difference between WT and *gckr* knockout RCC at 3 hpi (Fig. S1A and B). In addition, no differences in glycogen accumulation were found in both liver and muscle between WT and *gckr* knockout RCC (Fig. S1C and D). These observations indicate that *gckr* knockout also impairs postprandial gluconeogenesis but does not alter glycogen accumulation.

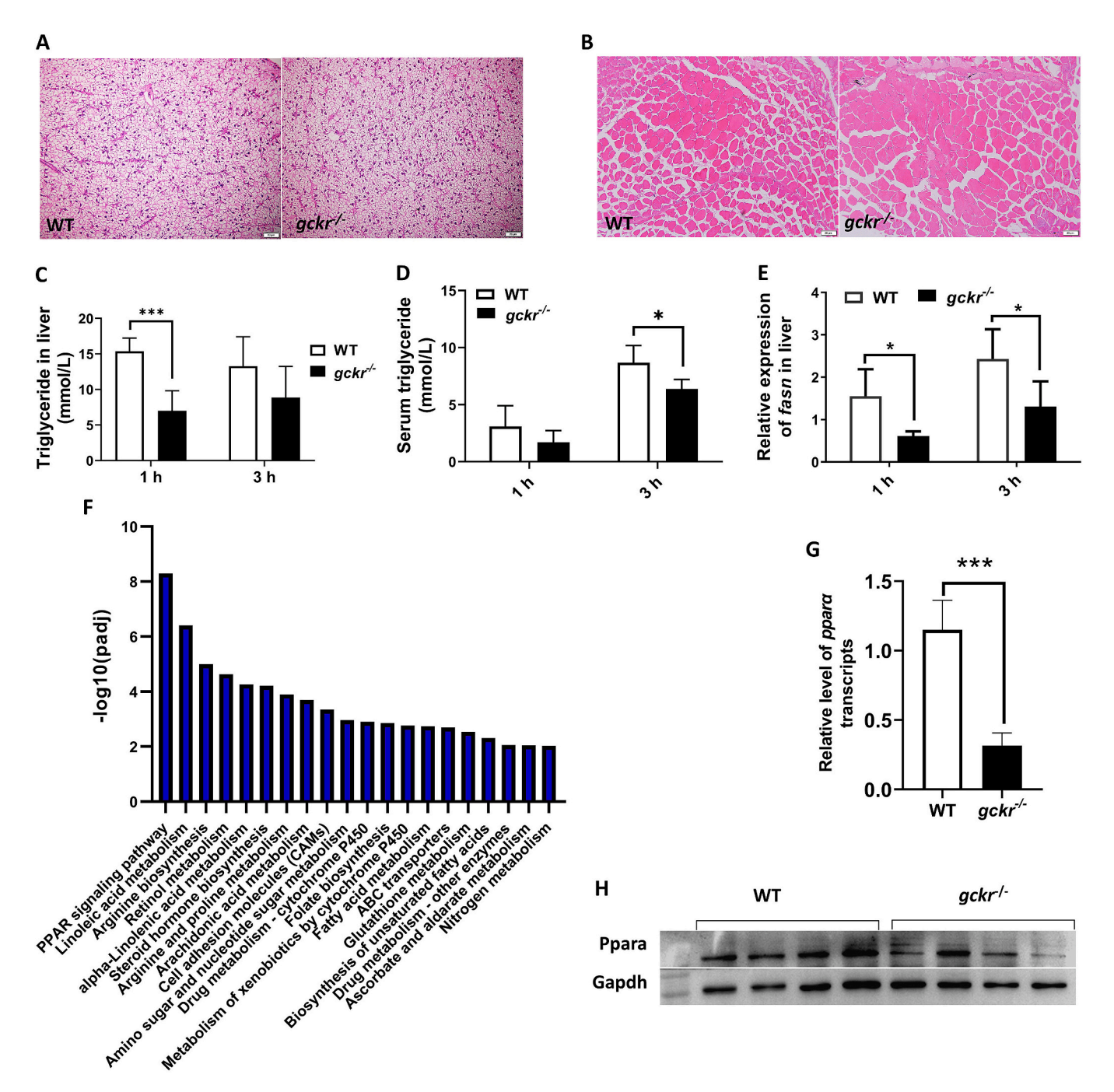


**Fig. 3.** Comparison of lipid metabolism between WT and *gckr* knockout RCC. (A) HE staining of livers from WT and *gckr* knockout RCC. (B) HE staining of muscle from WT and *gckr* knockout RCC. (C) Hepatic triglyceride contents between WT and *gckr* knockout RCC at 1 and 3 hpi. (D) Serum triglyceride levels between WT and *gckr* knockout RCC at 1 and 3 hpi. (E) Expression of *fasn* in livers of WT and *gckr* knockout RCC at 1 and 3 hpi. (F) KEGG enrichment from transcriptome analysis between WT and *gckr* knockout RCC. (G) Levels of hepatic *ppara* transcripts in WT and *gckr* knockout RCC at 1 hpi. (H) Western blot analysis of hepatic protein Ppara with Gapdh as the reference.

# 3.3. Gckr depletion reduced postprandial hepatic triglyceride synthesis and fat oxidation metabolism in RCC

Glycolysis is closely related to lipid metabolism, as the intermediate products of glycolysis can be converted into triglycerides. Therefore, it's necessary to investigate the status of lipid metabolism in gckr knockout RCC. HE staining was used to examine the morphology of liver and muscle in WT and gckr knockout RCC on a normal diet. It was found that the hepatocytes of both groups were round or oval, with nuclei in the centre, and there were no significant differences in the size of the hepatocytes and the density of hepatocytic nuclei between WT and gckr knockout RCC (Fig. 3A). Meanwhile, the morphology and density of muscle fiber bundles were also similar in the two groups (Fig. 3B). These results imply that gckr knockout doesn't affect fat accumulation under the normal diet. Subsequently, the postprandial triglyceride levels were determined in various tissues using triglyceride detection kit. Both WT and gckr knockout RCC exhibited a slight variation in hepatic triglyceride content from 1 to 3 hpi. However, gckr knockout RCC had significantly reduced triglyceride contents at 1 hpi, but similar triglyceride levels at 3 hpi compared to WT RCC (Fig. 3C). Correspondingly, gckr knockout RCC also exhibited significantly reduced serum triglyceride levels at 3 hpi (Fig. 3D). Furthermore, gckr knockout RCC also displayed dramatically downregulated expression of fatty acid synthase (fasn) at both 1 and 3 hpi (Fig. 3E). Additionally, the transcriptome analysis further revealed gckr knockout RCC had enriched PPAR signaling pathway at 1 hpi (Fig. 3F). The ppara transcripts and Ppara levels, which played an important role in lipid oxidation metabolism, were dramatically decreased in gckr knockout RCC (Fig. 3G and H). The above results

indicate that gckr knockout leads to a reduction in postprandial lipid synthesis and fat oxidation metabolism.

## 3.4. Gckr depletion resulted in increased visceral mass in RCC under a high-lipid diet

Considering that gckr knockout resulted in attenuated fat oxidation metabolism in RCC, it's necessary to examine its tolerance to high-lipid diets. We performed a feeding trial with a diet containing 8.8% lipid. After eight weeks of mixed culture, WT and gckr knockout RCC were identified by sequencing the gckr knockout target. It was found that the gckr knockout RCC exhibited a bulging abdomen, which was obviously thicker from the ventral view compared to WT RCC (Fig. 4A and B). Anatomically, both female and male gckr knockout RCC showed enlarged liver and excessive gonadal fat (Fig. 4C and D). After isolation, it was found that gckr knockout RCC showed obviously larger visceral masses than WT RCC (Fig. 4E). Moreover, gckr knockout RCC exhibited a significant increase in the weight of the visceral mass compared to WT RCC (Fig. 4F). In addition, the growth of gckr knockout RCC was also reduced under the high-lipid diet, with a significantly lower terminal body weights, even starting from the same initial weights (Fig. 4G). Similar to the observations on the normal diet, gckr knockout RCC had significantly lower serum insulin and pyruvate levels at 1 hpi (Fig. 4H and I). These results suggest that impaired insulin signaling and glycolysis are maintained in gckr knockout RCC under a high-lipid diet.

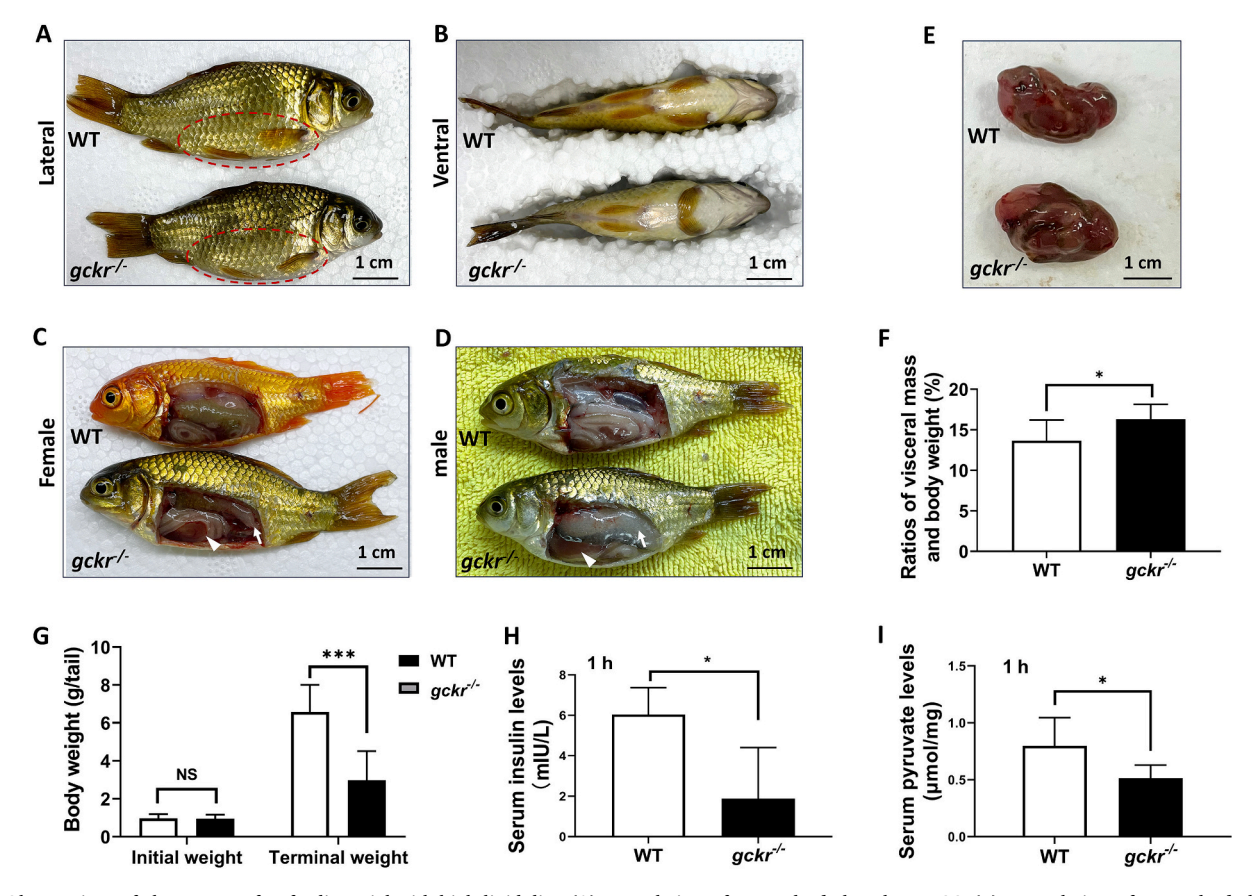


**Fig. 4.** Observations of phenotypes after feeding trial with high-lipid diet. (A) Lateral view of WT and *gckr* knockout RCC. (B) Ventral view of WT and *gckr* knockout RCC. (C) Anatomical observations of WT and *gckr* knockout females after high-lipid diet. (D) Anatomical observations of WT and *gckr* knockout males after high-lipid diet. The arrow and arrowhead in C and D indicate gonadal fat and enlarged liver in *gckr* knockout RCC. (E) Comparison of visceral mass between WT and *gckr* knockout RCC after high-lipid diet. (F) Statistic analysis of the proportions of visceral mass to body weight between WT and *gckr* knockout RCC. (G) Statistic analysis of initial body weight and terminal body weight of WT and *gckr* knockout RCC during the feeding trail with high-lipid diet. (H) Serum insulin levels in WT and *gckr* knockout RCC at 1 hpi. I) Serum pyruvate contents in WT and *gckr* knockout RCC at 1 hpi.

#### 3.5. Gckr depletion caused visceral obesity in RCC under a high-lipid diet

The increased visceral mass may indicate increased fat deposition in *gckr* knockout RCC. Therefore, we further examined the histological structure and fat content in the livers. HE staining showed that many vacuoles were present in the livers of six WT RCC examined, whereas

only two *gckr* knockout RCC had hepatic vacuoles and the other four *gckr* knockout RCC exhibited normal hepatic morphology (Fig. 5A and B). However, the oil red staining revealed that *gckr* knockout RCC exhibited obviously enriched stained lipid droplets in the liver (Fig. 5C and D). Moreover, *gckr* knockout RCC had significantly higher levels of visceral triglyceride, hepatic triglyceride, and serum triglyceride compared to

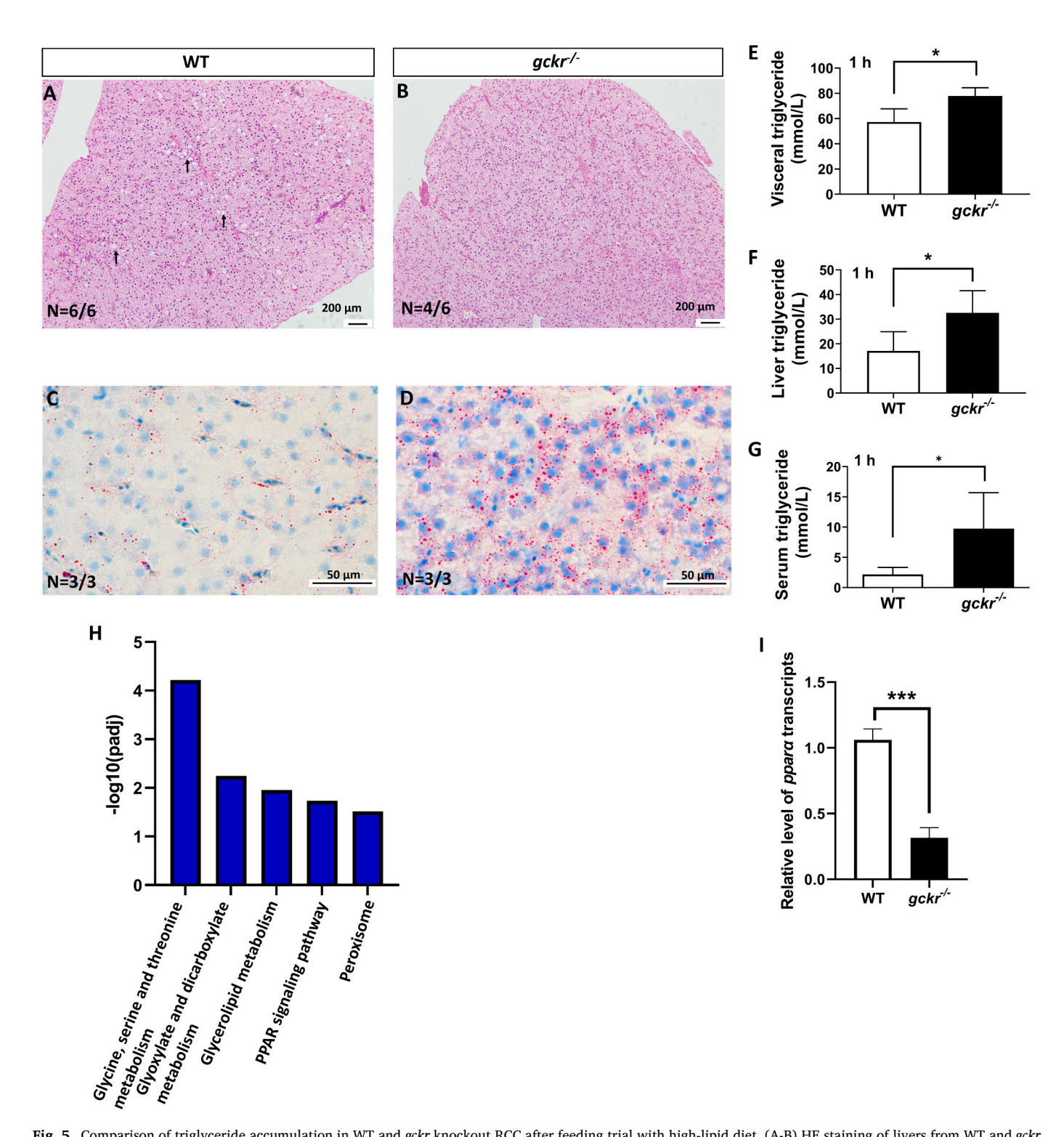


**Fig. 5.** Comparison of triglyceride accumulation in WT and *gckr* knockout RCC after feeding trial with high-lipid diet. (A-B) HE staining of livers from WT and *gckr* knockout RCC. (E) Visceral triglyceride contents in WT and *gckr* knockout RCC. (F) Hepatic triglyceride contents in WT and *gckr* knockout RCC. (G) Serum triglyceride levels in WT and *gckr* knockout RCC. (H) KEGG enrichment from transcriptome analysis between WT and *gckr* knockout RCC after high-lipid diet. (I) Levels of hepatic *ppara* transcripts at 1 hpi in WT and *gckr* knockout RCC after high-lipid diet. (For interpretation of the references to colour in this figure legend, the reader is referred to the web version of this article.)

WT RCC at 1 hpi (Fig. 5E-G). These results suggest that gckr knockout leads to increased fat deposition under the high-lipid diet. Based on the transcriptome analysis, it was revealed that gckr knockout RCC also maintained enriched PPAR signaling and decreased ppara transcripts (Fig. 5H and I). These results demonstrate that the increased fat deposition in gckr knockout RCC under high-lipid conditions may result from impaired lipid oxidation metabolism.

#### 4. Discussion

The current study demonstrates that Gckr plays an important role in promoting postprandial glycolysis and maintaining the balance between glucose and lipid metabolism in fish. For the first time, this study provides compelling evidence that Gckr may indirectly regulate insulin signaling, thereby further affecting growth and lipid metabolism. These findings highlight the importance of glycolysis in fish and provide a novel insight into improving growth performance in fish.

GCKR was identified as an inhibitor of glycolysis in mammalian hepatocytes by binding to GCK and thereby reducing the phosphorylation of glucose (Van Schaftingen, 1989; van Schaftingen et al., 1997). In this study, gckr knockout in RCC resulted in impaired serum glucose clearance and reduced GCK content (Fig. 2) during glucose tolerance. These results suggest that GCKR plays a role in the storage and protection of GCK in RCC. This finding is similar to the observations in GCKR mutant mice (Farrelly et al., 1999; Grimsby et al., 2000). Activation of GCK is a rate-limiting step in the induction of glycolysis (Ferre et al., 1996). The current study implies that gckr knockout leads to impaired glycolysis in RCC, supporting by compromised glucose clearance, decreased pk expression and subsequently reduced pyruvate levels after consuming glucose (Fig. 2). In glycolysis, GCK not only catalyzes the conversion of glucose to glucose 6-phosphate (G6P), which is the first rate-limiting step, but also regulates the last rate-limiting step by promoting the transcription of pk via G6P in hepatocytes (Matsuda et al., 1990). These data, taken together, suggest that the storage/protection function of Gckr promotes the postprandial glycolysis in RCC through maintaining GCK content and indirectly promoting pk expression.

Although GCKR in mice and RCC showed similar roles in GCK storage/protection, the downstream effects were distinctly different. Both reduced growth performance and serum insulin levels were only present in gckr knockout RCC (Farrelly et al., 1999; Grimsby et al., 2000). The poor growth performance in gckr mutant RCC may be due to impaired postprandial GCK levels, insulin levels, and insulin signaling (Fig. 1), as both reduced GCK levels and insulin levels/signaling have been reported to be associated with poor growth (Hattersley et al., 1998; Terauchi et al., 2000; Kitamura et al., 2003; Laron, 2008; Laron and Werner, 2020). Moreover, GCK has been reported to play a role in modulating glucose-stimulated insulin secretion (Efrat et al., 1994; Grupe et al., 1995; Terauchi et al., 1995; Sternisha and Miller, 2019; Chen et al., 2022;). These observations indicate that Gckr may indirectly regulate insulin secretion and growth through reciprocal control with Gck, while the underlying reasons for the discrepancies between mice and RCC in response to GCKR deficiency remains unknown.

GCK-mediated glucose phosphorylation is the rate-controlling step in insulin-stimulated hepatic glycogen synthesis *in vivo* (Nozaki et al., 2020). Activation of GCK can induced glycogen synthesis by increasing the intracellular concentration of glucose 6-phosphate (Ferre et al., 1996), while the inactivation of GCK resulted in a significant reduction in hepatic glycogen synthesis (Farrelly et al., 1999). However, no significant difference in hepatic glycogen deposition was observed between WT and *gckr* knockout RCC in this study (Fig. S1). This result may be attributed to reduced glycogenolysis, as glucose is considered to be the primary suppressor of hepatic glycogenolysis, and hyperglycemia is required to suppress glycogenolysis *in vivo* (Petersen et al., 1998; Petersen et al., 2017).

In mammals, GCK-regulated glucose disposal also promotes triglyceride synthesis by transforming excess carbohydrates to fatty acids and

activating the transcriptional activity of carbohydrate response element binding protein, which can promote the expression of Acc and Fasn (Towle et al., 1997; Li et al., 2010; Poupeau and Postic, 2011; Sternisha and Miller, 2019). Furthermore, lipogenesis is also transcriptionally controlled by sterol regulatory element-binding protein 1c (SREBP1c), which is directly activated by insulin signaling (Koo et al., 2001). In the current study, the knockout of gckr resulted in a reduction in postprandial triglyceride levels and fasn transcripts under a normal diet (Fig. 3). These results are consistent with the decreased GCK content and compromised insulin level/signaling in the gckr knockout RCC (Figs. 1 and 2). However, gckr knockout also impaired lipid oxidation by decreasing PPARa signaling (Figs. 3 and 5), which is known to promote  $\beta$ -oxidation in both hepatic and extrahepatic organs (Wang et al., 2020). Insulin was reported to enhance both the phosphorylation state and the transcriptional activity of PPARa (Desvergne and Wahli, 1999; Shalev et al., 1996). Consequently, our findings suggest that Gckr may indirectly promote lipogenesis and lipid oxidation through enhancing glycolysis and insulin signaling in RCC. Therefore, the fat accumulation in gckr knockout RCC mainly depended on the diet (Figs. 3 and 5). Significantly, the consumption of the high-lipid diet induced various metabolic syndrome traits in gckr knockout RCC, including increased visceral mass, hepatic fat accumulation, and an elevated plasma lipid profile (Figs. 4 and 5). These results demonstrate that gckr knockout reduces the tolerance to high-lipid diet in RCC. Although additional evidence is necessary to fully elucidate the potential involvement of Gckr in PPARa signaling, this study highlights the intricacies of lipid metabolism and underscores the essential role of Gckr in maintaining metabolic homeostasis in fish.

In summary, this study provides implications that enhancing glycolysis may promote growth and tolerance to high-lipid diet in fish.

#### 5. Conclusion

In this study, we generated *gckr* knockout RCC to investigate the resulting phenotype and metabolic characteristics. We found that *gckr* knockout resulted in diminished postprandial glycolysis. The impaired glycolysis in *gckr* knockout RCC further induced compromised insulin signaling, gluconeogenesis, lipogenesis and lipid oxidation metabolism. These metabolic alterations led to growth retardation and intolerance to high-lipid diets in *gckr* knockout RCC.

#### **Author statement**

We followed the laboratory animal guideline for the ethical review of the animal welfare of China (GB/T 35,892–2018). Before sampling, fish were euthanized with tricaine methanesulfonate (A5040-25G, Sigma) at a concentration of 100 mg/L. All animal experiments in this study were approved by the Institutional Animal Care and Use Committee of Hunan Normal University (Permit Number: 630).

#### CRediT authorship contribution statement

Juan Li: Writing – original draft, Methodology, Investigation, Formal analysis, Conceptualization. Huilin Li: Methodology, Investigation, Formal analysis, Conceptualization. Yuan Ou: Methodology, Investigation, Formal analysis. Qiyong Lou: Formal analysis, Conceptualization. Zehong Wei: Methodology, Data curation, Conceptualization. Ming Wen: Methodology, Data curation, Conceptualization. Shi Wang: Validation, Funding acquisition. Qingfeng Liu: Validation, Funding acquisition. Yuqin Shu: Writing – review & editing, Validation, Supervision, Resources, Methodology, Funding acquisition, Conceptualization. Shaojun Liu: Supervision, Resources.

#### Declaration of competing interest

The authors declare that they have no known competing financial

interests or personal relationships that could have appeared to influence the work reported in this paper.

#### Data availability

Data will be made available on request.

#### Acknowledgments

This work was supported by the National Natural Science Foundation of China (31802291), the Natural Science Foundation of Hunan Province (2021JJ40342, 2021JJ40343), and the Training Program for Excellent Young Innovators of Changsha (Grant No. kq2209013).

#### Appendix A. Supplementary data

Supplementary data to this article can be found online at https://doi.org/10.1016/j.aquaculture.2024.741245.

#### References

- Baur, F.J., Ensminger, L.G., 1977. The Association of Official Analytical Chemists (AOAC). J. Am. Oil Chem. Soc. 54, 171–172. https://doi.org/10.1007/BF02670789.
- Brown, K.S., Kalinowski, S.S., Megill, J.R., Durham, S.K., Mookhtiar, K.A., 1997. Glucokinase regulatory protein may interact with glucokinase in the hepatocyte nucleus. Diabetes 46, 179–186. https://doi.org/10.2337/diab.46.2.179.
- Chen, B., Du, Y.R., Zhu, H., Sun, M.L., Wang, C., Cheng, Y., Pang, H., Ding, G., Gao, J., Tan, Y., et al., 2022. Maternal inheritance of glucose intolerance via oocyte TET3 insufficiency. Nature 605, 761–766. https://doi.org/10.1038/s41586-022-04756-4.
- Desvergne, B., Wahli, W., 1999. Peroxisome proliferator-activated receptors: nuclear control of metabolism. Endocr. Rev. 20, 649–688. https://doi.org/10.1210/
- Detheux, M., Vandercammen, A., Van Schaftingen, E., 1991. Effectors of the regulatory protein acting on liver glucokinase: a kinetic investigation. Eur. J. Biochem. 200, 553–561. https://doi.org/10.1111/j.1432-1033.1991.tb16218.x.
- Efrat, S., Leiser, M., Wu, Y.J., Fusco-DeMane, D., Emran, O.A., Surana, M., Jetton, T.L., Magnuson, M.A., Weir, G., Fleischer, N., 1994. Ribozyme-mediated attenuation of pancreatic beta-cell glucokinase expression in transgenic mice results in impaired glucose-induced insulin secretion. Proc. Natl. Acad. Sci. USA 91, 2051–2055. https://doi.org/10.1073/pnas.91.6.2051.
- Enes, P., Panserat, S., Kaushik, S., Oliva-Teles, A., 2009. Nutritional regulation of hepatic glucose metabolism in fish. Fish Physiol. Biochem. 35, 519–539. https://doi.org/ 10.1007/s10695-008-9259-5
- Farrelly, D., Brown, K.S., Tieman, A., Ren, J., Lira, S.A., Hagan, D., Gregg, R., Mookhtiar, K.A., Hariharan, N., 1999. Mice mutant for glucokinase regulatory protein exhibit decreased liver glucokinase: a sequestration mechanism in metabolic regulation. Proc. Natl. Acad. Sci. USA 96, 14511–14516. https://doi.org/10.1073/ pnas 96 25 14511
- Ferre, T., Riu, E., Bosch, F., Valera, A., 1996. Evidence from transgenic mice that glucokinase is rate limiting for glucose utilization in the liver. FASEB J. 10, 1213–1218. https://doi.org/10.1096/fasebj.10.10.8751724.
- Grimsby, J., Coffey, J.W., Dvorozniak, M.T., Magram, J., Li, G., Matschinsky, F.M., Shiota, C., Kaur, S., Magnuson, M.A., Grippo, J.F., 2000. Characterization of glucokinase regulatory protein-deficient mice. J. Biol. Chem. 275, 7826–7831. https://doi.org/10.1074/jbc.275.11.7826.
- Grupe, A., Hultgren, B., Ryan, A., Ma, Y.H., Bauer, M., Stewart, T.A., 1995. Transgenic knockouts reveal a critical requirement for pancreatic beta cell glucokinase in maintaining glucose homeostasis. Cell 83, 69–78. https://doi.org/10.1016/0092-8674(95)90235-x.
- Hattersley, A.T., Beards, F., Ballantyne, E., Appleton, M., Harvey, R., Ellard, S., 1998. Mutations in the glucokinase gene of the fetus result in reduced birth weight. Nat. Genet. 19, 268–270. https://doi.org/10.1038/953.
- Jin, J., Yang, Y., Zhu, X., Han, D., Liu, H., Xie, S., 2018. Effects of glucose administration on glucose and lipid metabolism in two strains of gibel carp (*Carassius gibelio*). Gen. Comp. Endocrinol. 267, 18–28. https://doi.org/10.1016/j.ygcen.2018.05.023.
- Kitamura, T., Kahn, C.R., Accili, D., 2003. Insulin receptor knockout mice. Annu. Rev. Physiol. 65, 313–332. https://doi.org/10.1146/annurev.physiol.65.092101.142540.
- Koo, S.H., Dutcher, A.K., Towle, H.C., 2001. Glucose and insulin function through two distinct transcription factors to stimulate expression of lipogenic enzyme genes in liver. J. Biol. Chem. 276, 9437–9445. https://doi.org/10.1074/jbc.M010029200.
- Laron, Z., 2008. Insulin–a growth hormone. Arch. Physiol. Biochem. 114, 11–16. https://doi.org/10.1080/13813450801928356.
- Laron, Z., Werner, H., 2020. Insulin: a growth hormone and potential oncogene. Pediatr. Endocrinol. Rev. 17, 191–197. https://doi.org/10.17458/per.vol17.2020.lw. insulinghpotentialoncogene.

- Li, M.V., Chen, W., Harmancey, R.N., Nuotio-Antar, A.M., Imamura, M., Saha, P., Taegtmeyer, H., Chan, L., 2010. Glucose-6-phosphate mediates activation of the carbohydrate responsive binding protein (ChREBP). Biochem. Biophys. Res. Commun. 395, 395–400. https://doi.org/10.1016/j.bbrc.2010.04.028.
- Matsuda, T., Noguchi, T., Yamada, K., Takenaka, M., Tanaka, T., 1990. Regulation of the gene expression of glucokinase and L-type pyruvate kinase in primary cultures of rat hepatocytes by hormones and carbohydrates. J. Biochem. 108, 778–784. https://doi. org/10.1093/oxfordjournals.jbchem.a123280.
- Moon, T.W., 2001. Glucose intolerance in teleost fish: fact or fiction? Comp. Biochem. Physiol. B Biochem. Mol. Biol. 129, 243–249. https://doi.org/10.1016/S1096-4959 (01)00316-5
- Nozaki, Y., Petersen, M.C., Zhang, D., Vatner, D.F., 2020. Metabolic control analysis of hepatic glycogen synthesis in vivo. Proc. Natl. Acad. Sci. USA 117, 8166–8176. https://doi.org/10.1073/pnas.1921694117.
- Pautsch, A., Stadler, N., Löhle, A., Rist, W., Berg, A., Glocker, L., Nar, H., Reinert, D., Lenter, M., Heckel, A., et al., 2013. Crystal structure of glucokinase regulatory protein. Biochemistry 52, 3523–3531. https://doi.org/10.1021/bi4000782.
- Petersen, K.F., Laurent, D., Rothman, D.L., Cline, G.W., Shulman, G.I., 1998. Mechanism by which glucose and insulin inhibit net hepatic glycogenolysis in humans. J. Clin. Invest. 101, 1203–1209.
- Petersen, M.C., Vatner, D.F., Shulman, G.I., 2017. Regulation of hepatic glucose metabolism in health and disease. Nat. Rev. Endocrinol. 13, 572–587. https://doi. org/10.1038/nrendo.2017.80.
- Polakof, S., Míguez, J.M., Soengas, J.L., 2009. A hepatic protein modulates glucokinase activity in fish and avian liver: a comparative study. J. Comp. Physiol. B. 179, 643–652. https://doi.org/10.1007/s00360-009-0346-4.
- Poupeau, A., Postic, C., 2011. Cross-regulation of hepatic glucose metabolism via ChREBP and nuclear receptors. Biochim. Biophys. Acta 1812, 995–1006. https://doi. org/10.1016/j.bbadis.2011.03.015.
- Shalev, A., Siegrist-Kaiser, C.A., Yen, P.M., Wahli, W., Burger, A.G., Chin, W.W., Meier, C.A., 1996. The peroxisome proliferator-activated receptor alpha is a phosphoprotein: regulation by insulin. Endocrinology 137, 4499–4502. https://doi. org/10.1210/endo.137.10.8828512.
- Slosberg, E.D., Desai, U.J., Fanelli, B., St Denny, I., Connelly, S., Kaleko, M., Boettcher, B. R., Caplan, S.L., 2001. Treatment of type 2 diabetes by adenoviral-mediated overexpression of the glucokinase regulatory protein. Diabetes 50, 1813–1820. https://doi.org/10.2337/diabetes.50.8.1813.
- Sternisha, S.M., Miller, B.G., 2019. Molecular and cellular regulation of human glucokinase. Arch. Biochem. Biophys. 663, 199–213. https://doi.org/10.1016/j abb.2019.01.011.
- Tan, Q., Wang, F., Xie, S., Zhu, X., Lei, W., Shen, J., 2009. Effect of high dietary starch levels on the growth performance, blood chemistry and body composition of gibel carp (*Carassius auratus var. gibelio*). Aquac. Res. 40, 1011–1018. https://doi.org/ 10.1111/j.1365-2109.2009.02184.x.
- Terauchi, Y., Sakura, H., Yasuda, K., Iwamoto, K., Takahashi, N., Ito, K., Kasai, H., Suzuki, H., Ueda, O., Kamada, N., et al., 1995. Pancreatic beta-cell-specific targeted disruption of glucokinase gene. Diabetes mellitus due to defective insulin secretion to glucose. J. Biol. Chem. 270, 30253–30256. https://doi.org/10.1074/
- Terauchi, Y., Kubota, N., Tamemoto, H., Sakura, H., Nagai, R., Akanuma, Y., Kimura, S., Kadowaki, T., 2000. Insulin effect during embryogenesis determines fetal growth: a possible molecular link between birth weight and susceptibility to type 2 diabetes. Diabetes 49, 82–86. https://doi.org/10.2337/diabetes.49.1.82.
- Towle, H.C., Kaytor, E.N., Shih, H.M., 1997. Regulation of the expression of lipogenic enzyme genes by carbohydrate. Annu. Rev. Nutr. 17, 405–433. https://doi.org/10.1146/annurev.nutr.17.1.405.
- Van Schaftingen, E., 1989. A protein from rat liver confers to glucokinase the property of being antagonistically regulated by fructose 6-phosphate and fructose 1-phosphate. Eur. J. Biochem. 179, 179–184. https://doi.org/10.1111/j.1432-1033.1989. tb14538.x.
- van Schaftingen, E., Veiga-da-Cunha, M., Niculescu, L., 1997. The regulatory protein of glucokinase. Biochem. Soc. Trans. 25, 136–140. https://doi.org/10.1042/bst0250136
- Veiga-da-Cunha, M., Van Schaftingen, E., 2002. Identification of fructose 6-phosphate-and fructose 1-phosphate-binding residues in the regulatory protein of glucokinase. J. Biol. Chem. 277, 8466–8473. https://doi.org/10.1074/jbc.M105984200.
- Veiga-da-Cunha, M., Sokolova, T., Opperdoes, F., Van Schaftingen, E., 2009. Evolution of vertebrate glucokinase regulatory protein from a bacterial N-acetylmuramate 6phosphate etherase. Biochem. J. 423, 323–332. https://doi.org/10.1042/ bi20090986.
- Walton, M.J., Cowey, C.B., 1982. Aspects of intermediary metabolism in salmonid fish. Comp. Biochem. Physiol. 73, 59–79. https://doi.org/10.1016/0305-0491(82)90201-2.
- Wang, Y., Nakajima, T., Gonzalez, F.J., Tanaka, N., 2020. PPARs as metabolic regulators in the liver: lessons from liver-specific PPAR-null mice. Int. J. Mol. Sci. 21, 2061. https://doi.org/10.3390/ijms21062061.
- Wilson, R.P., 1994. Utilization of dietary carbohydrate by fish. Aquaculture 124, 67–80. https://doi.org/10.1016/0044-8486(94)90363-8.
- Zhang, C., Li, Q., Zhu, L., He, W., Yang, C., Zhang, H., Sun, Y., Zhou, L., Sun, Y., Zhu, S., et al., 2021. Abnormal meiosis in fertile and sterile triploid cyprinid fish. Sci. China Life Sci. 64, 1917–1928. https://doi.org/10.1007/s11427-020-1900-7.